PRELIMINARY TESTS OF THE REMS GT-SENSOR

Eduardo Sebastián and Javier Gomez-Elvira

Lab. de Robótica y Exploración Planetaria, Centro de Astrobiología, Ctra. Ajalvir Km.4, Torrejón de Ardoz, Spain
sebastianme@inta.es

Abstract: This paper describes and tests a mathematical model of the REMS GT-sensor (Ground Temperature), which will be part of the payload of the NASA MSL mission to Mars. A short review of the instrument most critical aspects like the in-flight calibration system and the small size, are presented. It is proposed a mathematical model of the GT-sensor based on an energy balance theory, which considers the internal construction of the thermopile, and allows the designer to model independently the change in any of its parameters. The instrument includes an in-flight calibration system which accounts for dust build up on the thermopile window during operations. Pre-calibration tests of the system are presented, demonstrating the good performance of the proposed model, as well as some required improvements.

1   INTRODUCTION

This paper describes a set of preliminary tests to validate a mathematical model of the REMS (Rover Environmental Mars Station) GT-sensor (Ground Temperature). The REMS is a meteorological station designed at the Centro de Astrobiología, which is part of the payload of the MSL (Mars Science Laboratory) NASA mission to Mars. This mission is expected to be launched in the final months of 2009. The detection of Mars surface temperature is essential to develop meteorological models of Mars atmospheric behavior (Richardson *et al.*, 2004). Mars suffers very extreme ground temperature gradients, from -135ºC to 40ºC between winter and summer. Also, differences of ±40ºC between the ground and the atmosphere at 1.5m over the surface are expected (Smith *et al.*, 2004).

The GT-sensor, as its name indicates, is dedicated to measure the brightness temperature of the Mars surface, using an infrared detector that measures the emitted thermal radiation. The detector focuses a large surface area, which is far enough from the rover as to minimize its influence, measuring the average temperature and avoiding local effects. The main GT-sensor requirement is to achieve an accuracy of 5K, in which the errors created by rover influence, ground emissivity uncertainty and sensor noise must be included.

The selected infrared detector is a thermopile. These sensors have the advantage that they can work at almost any operational temperature, are small and lightweight and comparative cheap, as well as they are sensible to all the infrared spectra. Taking into account the restricted resources available for the REMS, there is hardly any alternative to thermopiles. Contrary, thermopiles are not standard parts for space or military applications. Therefore, at present no formally space qualified thermopile sensors exist. It should be noted here, that the IRTM experiment on the VIKING mission and the MUPUS experiment of the ROSETA mission have proven the suitability of this kind of detector to measure low object temperatures under space conditions.

The paper is organized as follows; section 2 introduces a brief description the REMS GT-sensor. In section 3 the mathematical model of the sensor is presented. Section 4 shows preliminary real tests results, using the proposed model. Finally, section 5 summarizes the results.

2   THE REMS GT-SENSOR

The GT-sensor measures the emitted radiation of the Mars surface in two infrared wavelength channels, by using two detectors, looking directly to ground without any optical system. The selected measurement channels of the thermopiles are the 8-14μm and 16-20μm (Vázquez *et al.*, 2005). These channels avoid the abortion band of the CO_2 centred in 15μm (Martin, 1986), and minimize the influence

of sun radiation. The thermopiles are of the model TS-100 (IPHT, 2007), previously used for the ROSETA mission, which include a RTD sensor and a filter build to the specification and pre-bonded onto them as the thermopile window.

The use of two measurement channels is justified in two ways. First, each channel is specialised in the measure of a temperature range, based on the Planck law and higher S/N ratio. And second, the output signal of the two channels can be combined in order to apply colour pyrometry techniques. This can help to estimate the emissivity of the Mars ground, despite both channels appears to have nearly unit emissivity (Vázquez *et al.*, 2005).

The thermopiles are mounted inside a boom, figure 1, which is placed in the rover mast at 1.5m height. The boom has the form of a small arm of 150mm long, and it also hosts the electronics dedicated to amplify thermopiles signal. The boom is made of aluminium and is used as a thermal mass to ensure and acceptably low drift in thermopiles temperature. The boom's form permits to avoid the existence of lateral lobules in the thermopile FOV (field of view), minimizing the rover direct vision.

The GT-sensor includes an in-flight calibration system whose main goal is to compensate the detector degradation due to the deposition of dust over its window (Richardson *et al.*, 2004). The system is implemented, without moving parts, by a high emissivity, low mass calibration plate at a temperature of our choosing. It is placed in front of each detector, so that each detector looks at the ground through a hole in the plate. In this way the part of the FOV obstructed by the calibration system is an annulus, limiting the measurement solid angle.
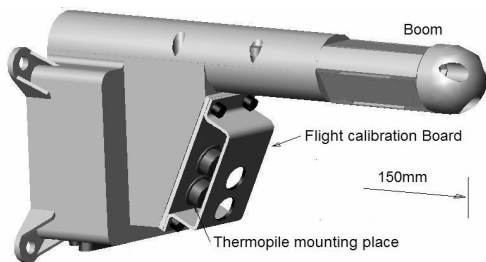

Figure 1: REMS boom and thermopile sensors.

3 MATHEMATICAL MODEL

Usually, the mathematical equation to model a thermopile considers it as a black box with an input, the incident energy, and an output, the output voltage. Therefore, a thermopile is characterised using a gain with units [V/W], which depends on thermopile temperature. This equation behaves

properly for high target temperatures, and when no thermopile worsening is expected during operation. Essentially, if there is degradation, a parameterized model is required in order to compensate it.

Contrary, the proposed model is based on an energy balance theory (Richardson *et al.*, 2004), which considers the internal thermopile structure and operation. It behaves better for low target temperatures, and for a wide range of thermopile temperatures. It also permits to establish adaptation algorithms for the change in model parameters.

3.1 Thermopile Model Equations

The proposed model uses two equations. The first one shows the response of the thermocouples, which form the thermopile. The thermopile is integrated by 100 thermocouples connected in series and embedded between the can and the bolometer (IPHT, 2007). The equation (1) determines the relation between the thermopile output voltage and the temperature difference between the hot (bolometer, T_s) and the cold junction (can, T_c). Therefore, from the measurement of (T_c) and the output voltage (V_{out}), the value of T_s can be obtained.

$$V_{out} = f(T_c)(T_s - T_c), \qquad (1)$$

The function $f(T_c)$ can be approximated by a polynomial expression provided by the thermopile manufacturer, which depends on thermopile or can temperature (T_c).

The second one is the energy balance equation, and it accounts for the heat fluxes into the thermopile bolometer from all the bodies around it. As the bolometer is designed to be well insulated from the can and to have low thermal mass, the equilibrium condition of the equation, is reached after a setting time of a few milliseconds. The equation considers a simplified model of energy exchange by thermal radiation (Q_R) and conduction (Q_C), see figure 2.
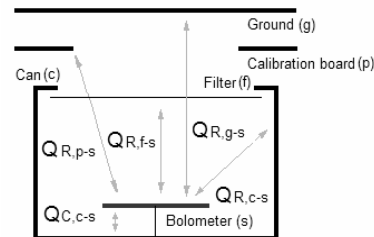

Figure 2: GT-Sensor energy terms.

From the analysis of the energy terms, and after the thermal equilibrium is reached, the equation (2) represents the thermal circuit

$$Q_{R,g-s} + Q_{R,p-s} + Q_{R,f-s} + Q_{R,c-s} + Q_{C,c-s} = 0 \quad (2)$$

Based on simplified heat flux models, the equation (2) can be expressed in the following way,

$$0 = (1-\alpha) K_1 \cdot (E_g^I - E_s^I) + \alpha \cdot K_1 \cdot (E_p^I - E_s^I) +$$
$$K_4 \cdot (E_f^O - E_s^O) + K_2 \cdot (E_c^T - E_s^T) + K_3 \cdot (T_c - T_s) \quad (3)$$

where α represents the factor of the thermopile FOV obstructed by the flight calibration board, and K_1, K_2, K_3 and K_4 are constants which modulate the weight of the different terms. These constants depend on physical factors of the bodies around like: emissivity, FOV factors, viewed areas, and in the case of K_3 on thermal conductance of the materials. The energy terms E_x^y are calculated integrating the Planck law (4) for each body temperature (T_x).

$$E_x^y = \int_{y1}^{y2} T(\lambda) \cdot 2hc^2 \Big/ \lambda^5 \cdot \left(e^{hc/\lambda K T_x} - 1 \right) d\lambda \quad (4)$$

where the subscript x represents the body, g(ground), p(calibration board), f(filter), c(thermopile can) and s(bolometer). $T(\lambda)$ is the transmittance of the filter. And the superscript T, I or O denotes if the energy flux is calculated in the total spectra, in band or out of filter band respectively.

3.2 Calibration System Equations

The main origin of thermopile degradation, while operating on Mars conditions, is dust deposition. During landed operations dust will collect on the thermopile's filter. Dust, which has high emisivity, will block light both into and out the detector, and it will equilibrate to the same temperature as the filter it is now in contact. It can therefore be seen as a changing the area of the filter into something similar to the can. In other words, if the factor β represent the part of the FOV that has not been obstructed by the dust, the equation (3) can be rewritten,

$$0 = \beta \cdot (1-\alpha) K_1 \cdot (E_g^I - E_s^I) + \beta \cdot \alpha \cdot K_1 \cdot (E_p^I - E_s^I) +$$
$$\beta \cdot K_1 \cdot (E_c^O - E_s^O) + (1-\beta) \cdot K_1 \cdot (E_c^T - E_s^T) +$$
$$K_2 \cdot (E_c^T - E_s^T) + K_3 \cdot (T_c - T_s) \quad (5)$$

The equation (5) includes two simplifications: The filter temperature is supposed to be equal to the can temperature, and the factor that weights the filter

influence K_4 is equal to the ground factor (K_1), due to both shares the same FOV.

Therefore, it is the factor β that must be determined during operations. This can be done by varying the temperature of the calibration board if the ground brightness temperature can be trust to remain constant while the temperature changed (Smith *et al.*, 2004). The temperature of the thermopile, the flight calibration board, and the output voltage of the thermopile must be collected before and after the temperature changed. Finally, using the data collected and the equation (5), the system of equations (6) can be defined,

$$0 = \beta \cdot \left[a \cdot E_g^I + b \cdot E_{p1}^I + c_1 \right] + d_1 \quad (6.1)$$
$$0 = \beta \cdot \left[a \cdot E_g^I + b \cdot E_{p2}^I + c_2 \right] + d_2 \quad (6.2)$$

where a, b, c and d are a set of known energy terms. And, the system can be solved for the factor β,

$$\beta = d_2 - d_1 \Big/ b \cdot (E_{p1}^I - E_{p2}^I) + c_1 - c_2 \quad (7)$$

4 TEST RESULTS

In this section, four preliminary experimental tests dedicated to validate and show the performance of the sensor model are presented. The tests pretend to be a simple exercise in ambient conditions of the experiments to calibrate the REMS GT-sensor.

Prior to start with the description of the tests, it is necessary to define the experiment setup, figure 3. A thermopile with a band past filter of 8-14μm, looking at the calibrated blackbody source MIKRON M315 and covering its all FOV, was used. The temperature of the flight calibration board and the thermopile's can have been measured using two individual T type thermocouples, glued to these elements. The temperatures of both elements have been controlled using two control systems CAL3200 and the associated thermocouple.
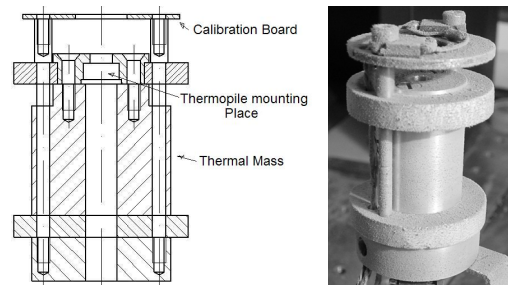

Figure 3: Thermopile model layout and real test model after dust deposition.

The first test tries to identify the value of those unknown constants of the thermopile model, table 1. In order to do it, different blackbody and thermopile temperatures were consigned, figure 4, while the flight calibration board was removed, which means that α is equal to 0. Therefore, based on the energy balance equation (2), where the energy terms are known, a least-squares problem for the tested points is established. Finally, the values of the constants, which minimize the least-squares error, are obtained.
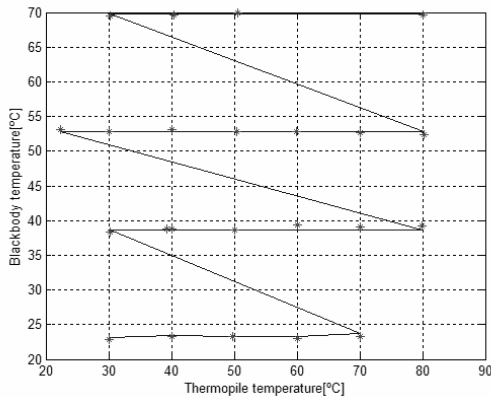

Figure 4: Real blackbody temperature (-) and estimated blackbody temperature (*) after the identification process.

Table 1: Thermopile and model variables.

Variable	Value
K_1	1
K_2	28.1695
K_3	128.4088W/K
$Error_{RMS}$	0.28K
α	0.34
Polynomial coefficients	[1.0826 -4.0577]
β	0.415

The second test has been carried out with the purpose of identifying the factor of the FOV obstructed by the flight calibration board, this is α. This value is an essential parameter, necessary for the flight calibration process.

During the test, the thermopile and the calibration board must be kept at ambient temperature, to ensure that their temperatures are homogeneous and stable. This requirement is necessary due to the radiance of the flight calibration has not previously calibrated, and in this way the error introduced by this factor is avoided. The blackbody temperature is set over the ambient temperature. In order to avoid the thermopile heating, due to the energy radiated by the blackbody, an opaque surface was introduced in between. This surface was removed during the measurement time

of bodies temperature and thermopile output. From these data, the energy terms of equation (2) were calculated, and we were able to solve for the values of α, for each blackbody temperature. Finally, these values of α were averaged in order to obtain a unique value, table 1.

The third test pretends to know the real temperature of the calibration board, which is required to calculate its real radiometric emission. The test consists of varying the flight calibration board temperature over the temperature of the thermopile, while the temperature of the thermopile and the blackbody are kept constant.

In this case, for each calibration board temperature, the blackbody and the thermopile temperatures were collected, as well as the thermopile's output. Therefore, based on these data and the energy valance equation (2), the radiometric emissions of the flight calibration board are derived, and from them the real temperatures, which were compared with the measured temperatures to determine the absolute calibration error, figure 5. Also, a first order polynomial, interpolating this error, has been obtained, table 1.
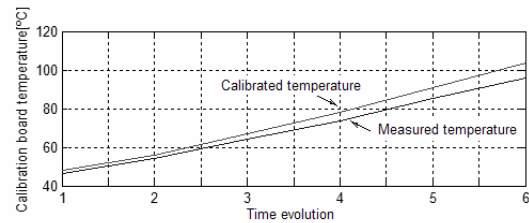

Figure 5: Temperature calibration error of the flight calibration board.

The final test is dedicated to analyse the behaviour of the in-flight calibration algorithm, after depositing a certain among of dust over the thermopile window, simulating Mars environment.

The test is divided in two different steps. In the first one, the flight calibration algorithm is run for different calibration board temperatures. The figure 6(Top) shows the obtained values of β, with and without considering the previous calibration of the calibration board. The data after calibration are more stable, validating this calibration and reducing algorithm error. As a result the average value of β is shown, table 1.

The second step is dedicated to measure the temperature of the blackbody from: the thermopile output, the calibrated thermopile model, the calculated value of the factor β due to dust deposition. During the test, the temperature of the blackbody was almost constant, while the

106

temperature of the thermopile was changed. Figure 6(bottom) shows the result after applying the measurement algorithm (5) and solving for T_g. The high temperature error is due to the flight calibration system is calibrating a small surface or annulus in the external part of the thermopile filter, while the filter surface used to measure the ground brightness temperature is in the middle, and the deposition appears to be no homogeneous. Thus, the obstruction factor β is higher than the real one.
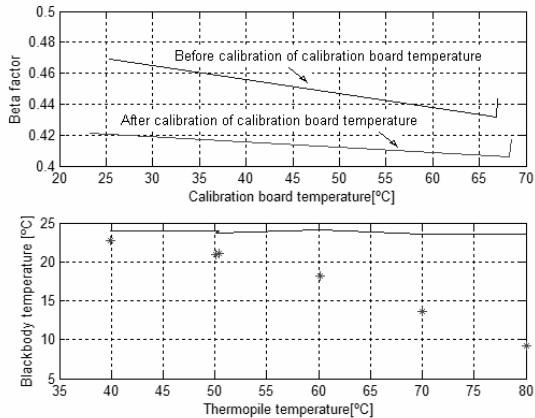

Figure 6: (top)Value of β factor. (bottom)Real blackbody temperature (-), and measured blackbody temperature (*).

5   CONCLUSIONS

The thermopile mathematical model presented in this paper is a valid and precise method to characterize a thermopile, due to the low least-squares error of 0.28K for an extensive thermopile temperature range of almost 60K.

The FOV obstruction factor, generated by the flight calibration board, reaches a value of 34%. It can be reduced in order to increase the S/N ratio for ground temperature signals.

The radiometric calibration of the flight calibration board is necessary due to the error introduced by different factors: the calibration of the temperature sensor, the temperature homogeneity of the calibration board and the position and anchoring of the temperature sensor.

Dust deposition, based on dust electrical characteristics, tends to form small balls around the union between the thermopile can and window. This is exactly the area calibrated by the flight calibration board, justifying the higher value of β. As a future work, a new calibration system, using a heated cable, will be studied. The cable will cross the FOV of the thermopiles, obstructing a homogenous part of the FOV, and not only a ring in the most external part. This will minimize the error generated by the way dust is built up on the window.

ACKNOWLEDGEMENTS

REFERENCES

Richardson M., McEwan I., Schofield T., Smith M. Souères P., Courdesses M. and Fleury S. 2004. MIDAS Mars Ice Dust Atmospheric Sounder. *MSL proposal.*

Vázquez L., Zorzano M.P., Fernández D., McEwan I. 2005. Considerations about the IR Ground Temperature Sensor. *CAB, REMS Technical Note 1-101722005.* Madrid.

Smith M.D. *et al.*, 2004. First Atmospheric Science Results from the Mars Exploration Rovers Mini.-TES. *SCIENCE EEE, 306*, 1750-1753.

Martin T.Z. 1986. Thermal infrared Opacity Of The Mars Atmosphere. *Icarus, 66*, 2-21.

www.ipht-jena.de. 2007. IPHT web page.